Contents

Todo list

Introduction 1

Quantum Materials

The United Nations declared 2025 the 'International Year of Quantum Science and Technology' [1]. This is an effort is to raise awareness of the importance of quantum science and its applications, which focuses in 3 key areas: quantum computing, quantum communications and quantum sensors.

One effect underlying many of these applications is the phenomenon of superconductivity. It was discovered in 1911, when Heike Onnes measured that the electrical resistance of Mercury suddenly vanished completely when cooling it below around 4 K [2].

While the mechanisms of superconductivity are not fully known in all cases, it is

As such, superconductivity is one of the important examples of quantum mechanical effects (i.e. the pairing of electrons) manifesting on a macroscopical scale. This makes it

High-Temperature Superconductivity

1986 and 1987: discovery of superconductivity with very high T_C found in cuprates [3, 4]. Cuprate superconductors are made up of layers of cooper oxide and charge reservoirs in between. The specific charge reservoir layers determine the properties of the SC and varying them lead to a rich zoo of materials with high T_C [5].

Largest commercial application to date is in magnetic resonance imaging, a medical technique using strong magnetic fields and field gradients [6]. Enabled due to the fact, that SCs can carry much stronger currents and thus generate much higher magnetic field strength. Technical applications in research are much wider, ranging from strong superconducting magnets in the LHC [7, 8] and other particle accelerators over detectors of single photons in astrophysics [9] to extremely sensitive measurement devices for magnetic fields [10] and voltages [11] based on the Josesphon effect [12].

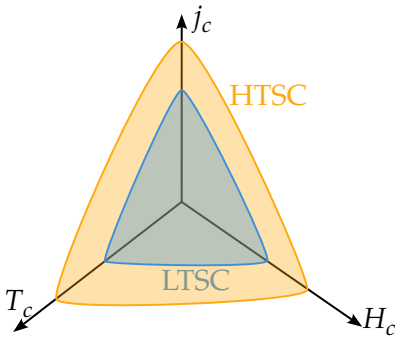

Figure 1.1 – Critical surface of a superconductor.

Since the first discovery of SC in cuprates, there has been a lot of work to develop superconductors with higher transition temperatures.

Flat Bands: Pairing and Supercurrent

A

Twisted Bilayer Graphene

One interesting development in is in twisted multilayer systems, first realized as twisted bilayer Graphene [13]. In comparison to the complex crystal structure of e.g. the Cuprates, twisted multilayer systems have a very simple structure and can be tuned very easily: the angle of twist between the layers can be easily accessed experimentally. The defining feature of these systems are flat electronic bands due to folding of the Brilluoin zone. Superconductivity in these systems is enhanced due to the fact that in the flat bands, interactions between the electrons are very strongly enhanced. Thus these systems are a very interesting playground to study strongly correlation effects in general and superconductivity in particular.

Organization of this thesis

2 Superconductivity

Superconductivity is an example of an emergent phenomenon: the Schrödinger equation describing all interactions between electrons gives no indication that there exists parameters for which the electrons condense into phase coherent pairs. In this chapter I review theoretical concepts needed for understanding superconductivity and introduce the tools used to study superconductivity in the later chapters. There are many textbooks covering these topics which can be referenced for a more detailed treatment, such as refs. [14–18].

Macroscopically, the superconducting state can be described by a spontaneous breaking of a $U(1)$ phase rotation symmetry that is associated with an order parameter. The theory of spontaneous symmetry breaking and associated phase transitions is Ginzburg-Landau theory discussed in section 2.1, following refs. [14, 19]. Ginzburg-Landau theory introduces two length scales: the coherence length ξ_0 describing the length scale of amplitude variations of the order parameter and the London penetration depth λ_L, which is connected to energy cost of phase variations of the order parameter. They also connect to the energy gap Δ and the condensate stiffness D_S, which are often competing energy scales in superconductors. The interplay of these length (energy) scales determine the macroscopic properties of a superconductors, so there is a great interest in accessing them in computational ways. To this end, section 2.1 also introduces a theoretical framework based on Cooper pairs with finite momentum [20] that will be used in later chapters to calculate these length scales from microscopic theories.

Ginzburg Landau theory is a macroscopic theory, but it can be connected to microscopic theories: if a theory finds an expression for the order parameter describing the breakdown of symmetry, it can be connected to quantities expressed by Ginzburg-Landau theory. One such theory to describe superconductivity from a microscopic perspective is BCS (Bardeen-Cooper-Schrieffer) theory in section 2.2, which is A method to treat local interactions non-perturbatively is DMFT (Dynamical Mean Field Theory). Section 2.4 briefly introduces the Greens function method to treat many-body problems and outlines the DMFT self-consistency cycle.

Furthermore, section 2.5 introduces an emerging perspective in the study of novel superconductors: it turns out that the superfluid weight is connected to a quantity of the electronic band structure called the quantum metric [21, 22], which is connected to

2.1 Ginzburg-Landau Theory of Superconductivity

Spontaneous Symmetry Breaking and Order Parameter

Symmetries are a powerful concept in physics. Noethers theorem [23] connects the symmetries of physical theories to associated conservation laws. An interesting facet of symmetries in physical theories is the fact, that a ground state of a system must not necessarily obey the same symmetries of its Hamiltonian, i.e. for a symmetry operation that is described by a unitary operator U, the Hamiltonian commutes with U (which results in expectation values of the Hamiltonian being invariant under the symmetry operation) but the states $|\phi\rangle$ and $U|\phi\rangle$ are different. This phenomenon is called spontaneous symmetry breaking and the state $|\phi\rangle$ is said to be symmetry-broken.

One consequence of this fact is that for a given symmetry-broken state $|\phi\rangle$, there exists multiple states that can be reached by repeatedly applying U to $|\phi\rangle$ and all have the same energy. To differentiate the symmetry-broken states an operator can be defined that has all these equivalent states as eigenvectors with different eigenvalues and zero expectation value for symmetric states. This is the microscopic notion of an order parameter.

The original notion of an order parameter was motivated from macroscopic observables that can then be related to the microscopic order parameter operator introduced above. Macroscopically I characterize the symmetry breaking by an order parameter Ψ which generally can be a complex-valued vector that becomes non-zero below the transition temperature T_C

$$|\Psi| = \begin{cases} 0 & T > T_C \\ |\Psi_0| > 0 & T < T_C \end{cases} . \tag{2.1}$$

In the example of a ferromagnet, a finite magnetization of a material is associated with a finite expectation value for the z-component of the spin operator, $m_z = \langle \hat{S}_z \rangle$. The order parameter describes the 'degree of order' [24]. Similarly to a magnetically ordered state, the SC state is characterized

by an order parameter. The theory of phase transitions in superconductors was developed by Ginzburg and Landau [25]. Landau theory and conversely Ginzburg-Landau theory is not concerned with the the microscopic properties of the order parameter, but describes the changes in thermodynamic properties of matter with the development of an order parameter. In superconductivity, the order parameter is described by coherent pairs of electrons with opposite momentum and spin. This will be explained in more detail later, but might be helpful to think of Cooper pairs already when discussing Ginzburg-Landau theory.

Landau and Ginzburg-Landau Theory

The free energy is a thermodynamic quantity:

$$F = E - TS \tag{2.2}$$

with the energy of the system E, temperature T and entropy S. A system in thermodynamic equilibrium has minimal free energy. The fundamental idea underlying Landau theory is to write the free energy $F[\Psi]$ as function of the order parameter Ψ and expand it as a polynomial:

$$F_L[\Psi] = \int \mathrm{d}^d x f_L[\Psi] \,, \tag{2.3}$$

where

$$f_L[\Psi] = \frac{r}{2}\Psi^2 + \frac{u}{4}\Psi^4 \tag{2.4}$$

is called the free energy density. Provided the parameters r and u are greater than 0, there is a minimum of $f_L[\Psi]$ that lies at $\Psi = 0$. Landau theory assumes that at the phase transition temperature T_C the parameter r changes sign, so it can be written in first order as

Do minima first, then redefine r

$$r = a(T - T_C) \,. \tag{2.5}$$

Figure 2.1a shows the free energy as a function of a single-component, real order parameter Ψ and it illustrates the essence of Landau theory: there are two cases for the minima of the free energy f

$$\Psi = \begin{cases} 0 & T \geq T_C \\ \pm\sqrt{\frac{a(T_C - T)}{u}} & T < T_C \end{cases} \,, \tag{2.6}$$

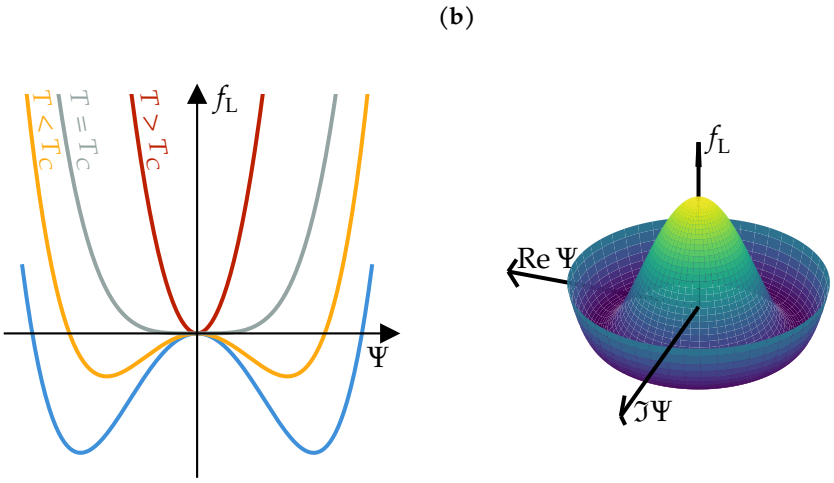

Figure 2.1 – Landau free energy and Mexican hat potential (a) Landau free energy f_L for a real-valued order parameter Ψ at different temperatures T. (b) Landau free energy for a complex order parameter Ψ.

so there is a for $T < T_C$ there are two minima corresponding to ground states with broken symmetry. When the order parameter can be calculated from some microscopic theory, the critical temperature T_C can be extracted from the behavior of the order parameter near T_C via a linear fit of

$$|\Psi|^2 \propto T_C - T \,. \tag{2.7}$$

Generalizing this from a one to an n-component order parameters is straightforward. One example is the complex or two component order parameter that will become important for superconductivity

$$\Psi = \Psi_1 + \mathrm{i}\Psi_2 = |\Psi| e^{\mathrm{i}\phi} \,. \tag{2.8}$$

The Landau free energy then takes the form

$$f_L[\Psi] = r\Psi^*\Psi + \frac{u}{2}(\Psi^*\Psi)^2 = r|\Psi|^2 + \frac{u}{2}|\Psi|^4 \tag{2.9}$$

with again

$$r = a(T_C - T) \,. \tag{2.10}$$

Instead of the two minima, the free energy here is rotational symmetry, because it is independent of the phase of the order parameter:

$$f_L[\Psi] = f_L[e^{i\phi}\Psi] \, . \tag{2.11}$$

This gives the so called 'Mexican hat' potential shown in fig. 2.1b. In this potential, the order parameter can be rotated continuously from one symmetry-broken state to another.

In 1950, Ginzburg and Landau published their theory of superconductivity, based on Landaus theory of phase transitions [25]. Where Landau theory as described above has an uniform order parameters, Ginzburg-Landau theory accounts for it being inhomogeneous, so an order parameter with spatially varying amplitude or direction. This in turn leads to the order parameter developing a fixed phase, which is the underlying mechanism of the superflow in superconductors.

Ginzburg-Landau theory can be developed for a general n-component order parameter, but in superfluids and superconductors the order parameter is complex, i.e. two-component. The Ginzburg-Landau free energy for a complex order parameter is

$$f_{\mathrm{GL}}[\Psi, \Delta\Psi] = \frac{\hbar^2}{2m^*}|\Delta\Psi|^2 + r|\Psi|^2 + \frac{u}{2}|\Psi|^4 \, , \tag{2.12}$$

where the gradient term $\Delta\Psi$ is added in comparison to the Landau free energy. The prefactor $\frac{\hbar^2}{2m^*}$ is chosen to illustrate the interpretation of the Ginzburg-Landau free energy as the energy of a condensate of bosons, where the gradient term $|\Delta\Psi|^2$ is the kinetic energy. The free energy in eq. (2.12) is sensitive to a twist of the phase of the order parameter. Substituting the expression $\Psi = |\Psi|e^{i\phi}$, the gradient term reads

$$\Delta\Psi = (\Delta|\Psi| + i\,\Delta\phi|\Psi|)e^{i\phi} \, . \tag{2.13}$$

With that, eq. (2.12) becomes

$$f_{GL} = \frac{\hbar^2}{2m^*}|\Psi|^2(\Delta\phi)^2 + \left[\frac{\hbar^2}{2m^*}(\Delta|\Psi|)^2 + r|\Psi|^2 + \frac{u}{2}|\Psi|^4\right] \, . \tag{2.14}$$

Now the contributions of phase and amplitude variations are split up: the first term describes energy cost of variations in the phase of the order parameter

and the second term describes energy cost of variations in the magnitude of the order parameter.

The dominating fluctuation is determined by the ratio of the factors $\frac{\hbar^2}{2m^*}$ and r, which has the dimension Length^2, from which define the correlation length.

$$\xi = \sqrt{\frac{\hbar^2}{2m^*|r|}} = \xi_0 \left(1 - \frac{T}{T_C}\right)^{-\frac{1}{2}} \tag{2.15}$$

where I define the zero temperature value as the coherence length $\xi_0 = \xi(T = 0) = \sqrt{\frac{\hbar^2}{2maT_C}}$. On length scales above ξ, the physics is entirely controlled by the phase degrees of freedom, i.e.

$$f_{\mathrm{GL}} = \frac{\hbar^2}{2m^*}|\Psi|^2 \left(\Delta\phi\right)^2 + \text{const.} \tag{2.16}$$

$$= \frac{\hbar^2}{4m^*} n_{\mathrm{S}} \left(\Delta\phi\right)^2 + \text{const.} \tag{2.17}$$

$$= D_{\mathrm{S}} \left(\Delta\phi\right)^2 + \text{const.} \tag{2.18}$$

where $\frac{n_{\mathrm{S}}}{2} = |\Psi|^2$ is the density of single electrons that form the Cooper pairs, also called the superfluid or superconducting density. Equation (2.18) shows that twisting the phase of the condensate is associated with an energy cost. This energy cost is characterized by the superfluid phase stiffness D_{S}.

Assuming frozen amplitude fluctuations $\Delta|\Psi(\mathbf{r})| = 0$, the stationary point of eq. (2.14) is

$$|\Psi| = |\Psi_0|\sqrt{1 - \xi^2 |\Delta\phi(\mathbf{r})|^2}\,. \tag{2.19}$$

This shows that the superconducting order gets suppressed and eventually destroyed by short-ranged (below ξ) phase fluctuations. By introducing a particular form of phase fluctuations $\phi = \mathbf{q}\cdot\mathbf{r}$ into a microscopic model, it is possible to probe this breakdown of superconductivity and thus gain insight into the nature of superconductivity, in particular this gives access to ξ.

The discussion so far is valid for neutral superfluids, but superconductors are charged superfluids, so they couple to electromagnetic fields. The Ginzburg-Landau free energy with minimal coupling to an electromagnetic field is

$$f_{\mathrm{GL}}[\Psi, \mathbf{A}] = \frac{\hbar^2}{2m^*}\left|\left(\Delta - \frac{\mathrm{i}e^*}{\hbar}\mathbf{A}\right)\Psi\right|^2 + r|\Psi|^2 + \frac{u}{2}|\Psi|^4 + \frac{B^2}{2\mu_0}\,. \tag{2.20}$$

with an additional term to include the electromagnetic energy of the magnetic field $\mathbf{B} = \nabla \times \mathbf{A}$. It really describes two intertwined Ginzburg-Landau theories for Ψ and $\mathbf{A}$. This mean there are two length scales, the coherence length ξ governing amplitude fluctuations of Ψ and the London penetration depth λ_L which determines the distance magnetic fields penetrate into the superconductor.

The current density can be calculated from the stationary point condition of the free energy w.r.t. the vector potential $\mathbf{A}$

$$\frac{\delta f_{\mathrm{GL}}}{\delta \mathbf{A}} = -\mathbf{j} + \frac{1}{\mu_0} \nabla \times \mathbf{B} \stackrel{!}{=} 0 \tag{2.21}$$

defining the supercurrent density

$$\mathbf{j} = -\mathrm{i}\frac{e\hbar}{m^*} \left(\Psi^* \Delta\Psi - \Psi \Delta\Psi^*\right) - \frac{4e^2}{m^*} |\Psi|^2 \mathbf{A} \,. \tag{2.22}$$

Introducing the order parameter with a fixed phase $\Psi = |\Psi| e^{\mathrm{i}\phi}$ gives

$$\mathbf{j} = 2e|\Psi|^2 \frac{\hbar}{m^*} \left(\nabla\phi - \frac{2\pi}{\Phi_0}\mathbf{A}\right) \tag{2.23}$$

with the magnetic flux quantum $\Phi_0 = \frac{\pi\hbar}{e}$. This shows that not only an applied field $\mathbf{A}$ can induce a supercurrent, but also the phase twist $\nabla\phi$ of the condensate ground state, which is the remarkable property of superconductors enabling the dissipationless current. Where a conventional current is achieved by excitations above the ground state, the superflow is achieved through deformation of the ground-state phase. The supercurrent can be gauge-transformed to

$$\mathbf{j} = -\frac{4e^2 n_S}{m^*}\mathbf{A} = \tilde{D}_S \mathbf{A} \tag{2.24}$$

which shows that the superfluid phase stiffness

$$D_{\mathrm{S}} = \frac{\hbar^2}{(2e)^2}\tilde{D}_S \tag{2.25}$$

also encodes the linear response of a system to a small applied vector field $\mathbf{A}$.

Connection of SF weight and London penetration depth

Superconducting Length Scales

As already discussed in the last section, access to the breakdown of the order parameter with phase fluctuations can give information on the coherence length ξ and the London penetration depth λ_L. This is a method developed by Witt et al. for characterizing superconductivity in alkali-doped fullerides, a material with strong electronic correlations. The authors find that multiorbital effects enable a superconducting state with a short coherence length but robust stiffness and a domeless rise in critical temperatures with increasing pairing interaction [20]. Access to the superconducting length scales is especially important in the context of BCS-BEC crossover physics and characterizing new high T_C superconductors. This is discussed in section 2.3.

This section gives an introduction to the method in Ginzburg-Landau theory, the inclusion into microscopic theories like BCS-theory and DMFT will be discussed in the respective sections.

Work over paragraph

As already discussed in the context of eq. (2.19), strong phase fluctuations destroy superconducting order. A particular choice of phase fluctuations would be

$$\phi(\mathbf{r}) = \mathbf{q} \cdot \mathbf{r} \tag{2.26}$$

which corresponds to Cooper pairs with a finite momentum $\mathbf{q}$.

In most materials: Cooper pairs do not carry finite center-of-mass momentum. In presence of e.g. external fields or magnetism: SC states with FMP might arise [26–28]

Procedure in the paper: enforce FMP states via constraints on pair-center-of-mass momentum $\mathbf{q}$, access characteristic lenght scales ξ_0, λ_L through analysis of the momentum and temperature-dependent OP. FF-type pairing with Cooper pairs carrying finite momentum:

$$\Psi_{\mathbf{q}}(\mathbf{r}) = |\Psi_{\mathbf{q}}| e^{i\mathbf{q}\mathbf{r}} \tag{2.27}$$

Then the free energy density eq. (2.12) is

$$f_{GL}[\Psi_{\mathbf{q}}] = r|\Psi_{\mathbf{q}}|^2 + \frac{u}{2}|\Psi_{\mathbf{q}}|^4 + \frac{\hbar^2 q^2}{2m^*}|\Psi_{\mathbf{q}}|^2 \tag{2.28}$$

Stationary point of the system:

$$\frac{\delta f_{GL}}{\delta \Psi^*_{\mathbf{q}}} = 2\Psi_{\mathbf{q}} \left[r(1 - \xi^2 q^2) + u|\Psi_{\mathbf{q}}|^2 \right] = 0 \tag{2.29}$$

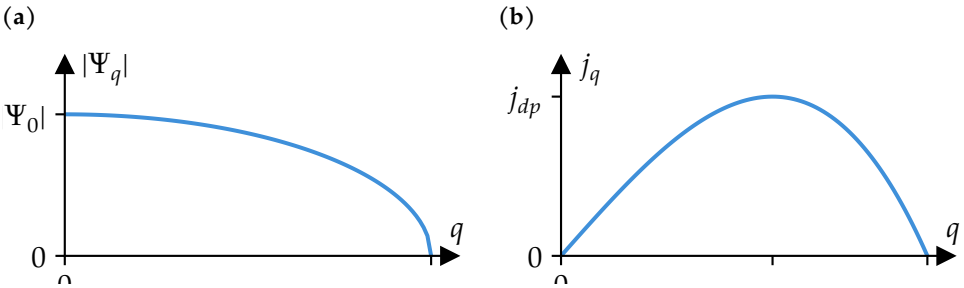

Figure 2.2 – Breakdown of the order parameter with larger q and superconducting current in Ginzburg-Landau theory. (a). (b)

which results in the **q**-dependence of the OP

$$|\Psi_{\mathbf{q}}|^2 = |\Psi_0|^2 \left(1 - \xi(T)^2 q^2\right) \tag{2.30}$$

For some value, SC order breaks down, $\psi_{\mathbf{q}_c} = 0$, because the kinetic energy from phase modulation exceeds the gain in energy from pairing. In GL theory: $q_c = \xi(T)^{-1}$. The temperature dependence of the OP and extracted $\xi(T)$ gives access to the coherence length via eq. (2.15)

$$\xi(T) = \xi_0 \left(1 - \frac{T}{T_C}\right)^{-\frac{1}{2}} \tag{2.31}$$

The momentum of the Cooper pairs entails a charge supercurrent $\mathbf{j_q}$. The current coming from the momentum can be calculated from eq. (2.22) (using $\phi(\mathbf{r}) = \mathbf{q} \cdot \mathbf{r}$ and $\mathbf{A} = 0$):

$$\mathbf{j_q} = \frac{2\hbar e}{m^*} |\Psi_{\mathbf{q}}|^2 \mathbf{q} \tag{2.32}$$

The current $\mathbf{j_q}$ is a non-monotonous function of **q** with a maximum called the depairing current j_{dp} as can be seen in fig. 2.2b . The depairing current is an upper boundary for the maximal current that can flow through a material, also called the critical current $\mathbf{j}_c$. The value of $\mathbf{j}_c$ is strongly dependent on the geometry of the sample [29, 30], so $\mathbf{j}_{dp}$ is not necessarily experimentally available, but it can be used to calculate the London penetration depth [15]

Depairing current connected with correlation length and penetration depth

$$\lambda_L(T) = \sqrt{\frac{\Phi_0}{3\sqrt{3}\pi\mu_0 \xi(T) j_{\mathrm{dp}}(T)}} = \lambda_{L,0} \left(1 - \left(\frac{T}{T_C}\right)^4\right)^{-\frac{1}{2}} \tag{2.33}$$

The superfluid phase stiffness can then be calculated via

$$D_S \propto \lambda_L^{-2} \tag{2.34}$$

Where does this formula come from? Second London equation

The finite-momentum method in the limit of $\mathbf{q} \to 0$ is related to linear response techniques to calculate the superfluid weight [21, 31].

2.2 Bardeen-Coooper-Schrieffer Theory

The BCS (Bardeen-Cooper-Schrieffer) description of superconductivity describes superconductivity as the condensation of electrons into pairs that form a macroscopic quantum state. There exist many textbooks tackling BCS theory from different angles, such as refs. [14, 15]. This section gives an introduction to the relevant physics of BCS theory as originally proposed, then derives (BCS) mean-field theory for the multiband Hubbard model.

Better introduction

BCS Hamiltonian

Work over paragraph

BCS-Hamiltonian:

$$H_{\text{BCS}} = \sum_{\mathbf{k}\sigma} \epsilon_{\mathbf{k}\sigma} c^\dagger_{\mathbf{k}\sigma} c_{\mathbf{k}\sigma} + \sum_{\mathbf{k},\mathbf{k}'} V_{\mathbf{k},\mathbf{k}'} c^\dagger_{\mathbf{k}\uparrow} c^\dagger_{-\mathbf{k}\downarrow} c_{-\mathbf{k}'\downarrow} c_{\mathbf{k}'\uparrow} \tag{2.35}$$

This Hamiltonian can be solved exactly using a mean field approach, because it involves an interaction at zero momentum and thus infinite range. Order parameter in mean field BCS theory is the pairing amplitude

$$\Delta = -\frac{U}{N_{\mathbf{k}}} \sum_{\mathbf{k}} \langle c_{-\mathbf{k}\downarrow} c_{\mathbf{k}\uparrow} \rangle = -U \langle c_{-\mathbf{r}=0\downarrow} c_{\mathbf{r}=\mathbf{0}\uparrow} \rangle \simeq U\Psi \,. \tag{2.36}$$

A finite Δ corresponds to the pairing introduced above: there is a finite expectation value for a coherent creation/annihilation of a pair of electrons with opposite momentum and spin. A finite Δ also introduces a band gap into the spectrum. BCS theory brings multiple aspects together: concept of paired electrons with the pairing amplitude being the order parameter in SC, an explanation for the attractive interaction overcoming Coulomb repulsion and a model Hamiltonian that very elegantly captures the essential physics. In particular, the model Hamiltonian can be expanded with other types of pairing

interactions to give a picture of superconductivity in the cuprates, compare ch. 15 in [14].

BCS theory is very successful in two ways: on the one hand it could quantitatively predict effects in the SCs known at the time, for example the Hebel-Slichter peak that was measured in 1957 [32, 33] and the band gap measured by Giaever in 1960 [34]. On the other hand, it established electronic pairing, i.e. the picture of a quantum-mechanical wave function with a defined phase as already described by Fritz London in 1937 [35] as the microscopic mechanism behind SC. This picture still holds today even for high T_C/unconventional superconductors, so SCs that cannot be described by BCS theory [36].

Multiband BCS Theory

Write chemical potential properly

The Hubbard model is the simplest model for interacting electron systems. It goes back to works by Hubbard [37], Kanamori [38] and Gutzweiler [39] in the 1960s. The Hamiltonian of the single-band Hubbard model is

$$H = H_0 + H_{\text{int}} = \sum_{\langle ij\rangle\sigma} \left(-t_{i,j} - \mu_\sigma \delta_{i,j}\right) c^\dagger_{i,\sigma} c_{j,\sigma} + \text{h.c.} + U \sum_i c^\dagger_{i,\uparrow} c^\dagger_{i,\downarrow} c_{i,\downarrow} c_{i,\uparrow} \quad (2.37)$$

where $U > 0$. The interaction describes a repulsive interaction between electrons of different spin at the same lattice site.

The Hubbard model emphasizes the electronic correlations due to local interactions, but with the discovery of high T_C SC in the Cuprates, it was quickly realized that the 2D Hubbard model in the intermediate to strong-coupling regime could describe the CuO_2 layers [40] well. The Hubbard model has parameter regimes with i.e. $d_{x^2-y^2}$ superconductivity, strong antiferromagnetic correlations, stripes, pseudogaps, Fermi liquid, and bad metallic behavior, with the phase diagram lines and observables being similar as a function of doping and temperature. Besides the relevancy of the Hubbard model for the Cuprates, the character of the model as having few parameters and simultaneously a very rich phase diagram with a variety of many-body effects also made it a perfect playground for new numerical tools, among them diagonalization, diagrammatics, tensor network, Quantum Monte Carlo (QMC) methods and DMFT (see section 2.4) [41].

The Hubbard model in the form of eq. (2.37) can be extended in a multitude of ways to model a variety of physical system. Here: extension to multiple orbitals (i.e. atoms in the unit cell for lattice systems) and an attractive interaction,

i.e. a negative U. Physical motivation for taking a negative-U Hubbard model: electrons can experience a local attraction interaction, for example through electrons coupling with phononic degrees of freedom or with electronic excitations [42]. The form of the interaction term is then:

$$H_{\text{int}} = -\sum_{i,\alpha} U_\alpha c^\dagger_{i,\alpha,\uparrow} c^\dagger_{i,\alpha,\downarrow} c_{i,\alpha,\downarrow} c_{i,\alpha,\uparrow} \tag{2.38}$$

where α counts orbitals and the minus sign in front is taken so that $U > 0$ now corresponds to an attractive interaction (this is purely convention).

There are a multitude of ways to derive a mean field description of a given interacting Hamiltonian. Very rigorous in path integral formulations as saddle points, given for example in ref. [14]. The review follows ref. [43]. A more intuitive way based on ref. [16] discussed here looks at the operators and which one are small.

Look at interaction term eq. (2.38). Mean-field approximation: operators A do not deviate much from their average value $\langle A \rangle$, i.e. the deviation $\delta A = A - \langle A \rangle$ are small. Specifically for superconductivity i.e. pairing, the operators

$$d_{i,\alpha} = c^\dagger_{i,\alpha,\uparrow} c^\dagger_{i,\alpha,\downarrow} - \langle c^\dagger_{i,\alpha,\uparrow} c^\dagger_{i,\alpha,\downarrow} \rangle \tag{2.39}$$

$$e_{i,\alpha} = c_{i,\alpha,\downarrow} c_{i,\alpha,\uparrow} - \langle c_{i,\alpha,\downarrow} c_{i,\alpha,\uparrow} \rangle \tag{2.40}$$

are small (dont contribute much to expectation values and correlation functions). So that in the interaction part of the Hamiltonian

$$H_{\text{int}} = -\sum_{i,\alpha} U_\alpha c^\dagger_{i,\alpha,\uparrow} c^\dagger_{i,\alpha,\downarrow} c_{i,\alpha,\downarrow} c_{i,\alpha,\uparrow} \tag{2.41}$$

$$= -\sum_{i,\alpha} U_\alpha \left(d^\dagger_{i,\alpha} + \langle c^\dagger_{i,\alpha,\uparrow} c^\dagger_{i,\alpha,\downarrow} \rangle \right) \left(e_{i,\alpha} + \langle c_{i,\alpha,\downarrow} c_{i,\alpha,\uparrow} \rangle \right) \tag{2.42}$$

$$= -\sum_{i,\alpha} U_\alpha (d_{i,\alpha} e_{i,\alpha} + d_{i,\alpha} \langle c_{i,\alpha,\downarrow} c_{i,\alpha,\uparrow} \rangle + e_{i,\alpha} \langle c^\dagger_{i,\alpha,\uparrow} c^\dagger_{i,\alpha,\downarrow} \rangle + \langle c^\dagger_{i,\alpha,\uparrow} c^\dagger_{i,\alpha,\downarrow} \rangle \langle c_{i,\alpha,\downarrow} c_{i,\alpha,\uparrow} \rangle) \tag{2.43}$$

the first term is quadratic in the deviation and can be neglected. Thus arrive at the approximation

$$\begin{aligned} H_{\text{int}} \approx & -\sum_{i,\alpha} U_\alpha \left(d_{i,\alpha} \langle c_{i,\alpha,\downarrow} c_{i,\alpha,\uparrow} \rangle + e_{i,\alpha} \langle c^\dagger_{i,\alpha,\uparrow} c^\dagger_{i,\alpha,\downarrow} \rangle \right. \\ & \left. + \langle c^\dagger_{i,\alpha,\uparrow} c^\dagger_{i,\alpha,\downarrow} \rangle \langle c_{i,\alpha,\downarrow} c_{i,\alpha,\uparrow} \rangle \right) \qquad (2.44) \\ = & -\sum_{i,\alpha} U_\alpha \left(c^\dagger_{i,\alpha,\uparrow} c^\dagger_{i,\alpha,\downarrow} \langle c_{i,\alpha,\downarrow} c_{i,\alpha,\uparrow} \rangle + c_{i,\alpha,\downarrow} c_{i,\alpha,\uparrow} \langle c^\dagger_{i,\alpha,\uparrow} c^\dagger_{i,\alpha,\downarrow} \rangle \right. \\ & \left. - \langle c^\dagger_{i,\alpha,\uparrow} c^\dagger_{i,\alpha,\downarrow} \rangle \langle c_{i,\alpha,\downarrow} c_{i,\alpha,\uparrow} \rangle \right) \qquad (2.45) \\ = & \sum_{i,\alpha} \left(\Delta_{i,\alpha} c^\dagger_{i,\alpha,\uparrow} c^\dagger_{i,\alpha,\downarrow} + \Delta^*_{i,\alpha} c_{i,\alpha,\downarrow} c_{i,\alpha,\uparrow} - \frac{|\Delta_{i,\alpha}|^2}{U_\alpha} \right) \qquad (2.46) \end{aligned}$$

with the expectation value

$$\Delta_{i,\alpha} = -U_\alpha \langle c_{i,\alpha,\downarrow} c_{i,\alpha,\uparrow} \rangle \qquad (2.47)$$

which is called the superconducting gap and is the order parameter introduced in Ginzburg-Landau theory in section 2.1. This results in the mean-field Hamiltonian

$$H_{\text{MF}} = \sum_{\langle ij \rangle \sigma} \left(-t_{i,j} - \mu_\sigma \delta_{i,j} \right) c^\dagger_{i,\sigma} c_{j,\sigma} + \text{h.c.} + U \sum_i c^\dagger_{i,\uparrow} c^\dagger_{i,\downarrow} c_{i,\downarrow} c_{i,\uparrow} \qquad (2.48)$$

MF Hamiltonian, with chemical potential

To include finite momentum in BCS theory, take the ansatz of a Fulde-Ferrel (FF) type pairing [44]:

$$\Delta_{i,\alpha} = \Delta_\alpha e^{i\mathbf{q}\mathbf{r}_{i\alpha}} \qquad (2.49)$$

Using the Fourier transform (with position vectors $\mathbf{r}_{i\alpha} = \mathbf{R}_i + \delta_\alpha$, position of the unit cell $\mathbf{R}_i$ and position of the orbital inside the unit cell δ_α)

$$c_{i\alpha\sigma} = \frac{1}{\sqrt{N}} \sum_{\mathbf{k}} e^{i\mathbf{k}\mathbf{r}_{i\alpha}} c_{\mathbf{k}\alpha\sigma} \qquad (2.50)$$

can write mean-field Hamiltonian as

$$H_{\text{MF}}(\mathbf{q}) = \sum_{\mathbf{k}} \mathbf{C}^\dagger_{\mathbf{q},\mathbf{k}} H_{\text{BdG}}(\mathbf{q},\mathbf{k}) \mathbf{C}_{\mathbf{q},\mathbf{k}} + K_{\mathbf{q}} \qquad (2.51)$$

$$C_{\mathbf{q},\mathbf{k}} = \begin{pmatrix} c_{\mathbf{k}1\uparrow} & c_{\mathbf{k}2\uparrow} & \dots & c_{\mathbf{k}n_{\text{orb}}\uparrow} & c^\dagger_{\mathbf{q}-\mathbf{k}1\downarrow} & c^\dagger_{\mathbf{q}-\mathbf{k}2\downarrow} & \dots & c^\dagger_{\mathbf{q}-\mathbf{k}n_{\text{orb}}\downarrow} \end{pmatrix}^T \qquad (2.52)$$

$$K_{\mathbf{q}} = \sum_{\mathbf{k}} \text{Tr}[H^\downarrow_{\mathbf{k}}] - n_{\text{orb}} N \mu - N \sum_\alpha \frac{|\Delta_\alpha(\mathbf{q})|^2}{U} \qquad (2.53)$$

with the so-called Bogoliubov-de Gennes (BdG) matrix

$$H_{\mathrm{BdG}}(\mathbf{k}) = \begin{pmatrix} H^{\uparrow}_{\mathbf{q}+\mathbf{k}} - \mu & \Delta(\mathbf{q}) \\ \Delta^{\dagger}(\mathbf{q}) & -\left(H^{\downarrow}_{\mathbf{q}-\mathbf{k}}\right)^{*} + \mu \end{pmatrix} \tag{2.54}$$

with $H_{0,\sigma}$ being the F.T. of the kinetic term and

F.T. of kinetic term

$$\Delta = \mathrm{diag}(\Delta_1(\mathbf{q}), \Delta_2(\mathbf{q}), \dots, \Delta_{n_{\mathrm{orb}}}(\mathbf{q})) \,. \tag{2.55}$$

For time-reversal symmetric systems, there exists a solution s.t. all Δ_α are real [21]. The introduction of the $\mathbf{q}$ breaks time-reversal symmetry, s.t. in a multiband system, the order parameters in the orbital can develop different phases.

Problem is now reduced to diagonalization of the BdG matrix. Write

$$H_{\mathrm{BdG}} = U_{\mathbf{q},\mathbf{k}} \epsilon_{\mathbf{q},\mathbf{k}} U^{\dagger}_{\mathbf{q},\mathbf{k}} \tag{2.56}$$

and

$$H_{\mathrm{MF}} = \sum_{\mathbf{q},\mathbf{k}} \gamma_{\mathbf{q},\mathbf{k}} \epsilon_{\mathbf{q},\mathbf{k}} \gamma^{\dagger}_{\mathbf{q},\mathbf{k}} \tag{2.57}$$

with quasi-particle operators

$$\gamma_{\mathbf{q},\mathbf{k}} = U^{\dagger}_{\mathbf{q},\mathbf{k}} C_{\mathbf{q},\mathbf{k}} \tag{2.58}$$

Write indeces everywhere without comma

Using the gap equation

gap equation

$$\begin{aligned} \Delta_\alpha &= -U_\alpha \langle c_{i,\alpha,\downarrow} c_{i,\alpha,\uparrow} \rangle = -\frac{U}{N} \sum_{\mathbf{k}} \langle c_{\mathbf{q}+\mathbf{k}} \rangle \\ &= -\frac{U}{N} \\ &= -\frac{U}{N} \end{aligned} \tag{2.59}$$

the order parameter can be determined self-consistently, i.e. starting from an initial value, the BdG matrix needs to be set up, diagonalized and then used to determine Δ_α again, until a converged value is found.

SC current in BCS

2.3 The BCS-BEC Crossover

One of the challenges in achieving high-temperature superconductivity is the fact that the two intrinsic energy scales of superconductors i.e. the pairing amplitude and the phase coherence often compete. Can be seen in the phenomenon of BCS-BEC crossover physics [45]. The picture of this crossover is the following: for a small attractive interaction, pairs of electrons are very loosely bound and mobile, while for a stronger interaction the pairs are bound together stronger and are not mobile, because hopping of a pair would involve a virtual hopping, thus breaking up the pair. This is highly suppressed. The crossover region between these two regimes is the BCS-BEC crossover. The energy scales characterizing the crossover are the superconducting gap/order parameter describing how strong the order is and the superfluid weight describing how mobile the Cooper pairs are. These two energy scales are equivalently defined via the coherence length ξ_0 and the London penetration depth introduced in section 2.1.

Section about BCS-BEC crossover

2.4 Dynamical Mean-Field Theory

The foundational idea of Dynamical Mean Field Theory (DMFT) is to map the full interacting problem to the problem of a single lattice site (or a small cluster of lattice sites) embedded in a mean field encompassing all non-local correlation effects, as seen in fig. 2.3.

This

DMFT has

What is the basic idea of DMFT?

This section describes the method of Green's function, which is the language DMFT is formulated in, the mapping of the lattice problem onto the impurity problem and the resulting self-consistency loop of DMFT. Additionally, I will also briefly describe how to describe the superconducting state in terms of Green's function and the consequences for a DMFT implementation. I will not fully derive the equations of DMFT here, for a more (pedagogical) introduction see refs. [14, 16, 46, 47].

What has been achieved with DMFT

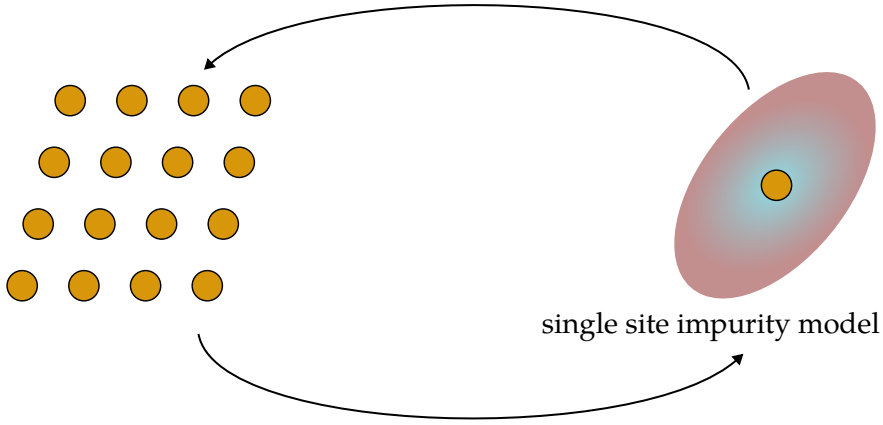

Figure 2.3 – Mapping of the full lattice problem . This also

Green's Function Formalism

Green's functions: method to encode influence of many-body effects on propagation of particles in a system. Depending on the context, different kinds of Green's functions are employed. For exampple, Matsubara Green's functions naturally includes finite temperatures. This is done via a so-called Wick rotation of the time variable t into imaginary time

$$t \to -\mathrm{i}\tau \tag{2.60}$$

where τ is real and has the dimension time. This enables the simultaneous expansion of exponential $e^{-\beta H}$ coming from the thermodynamic average and $e^{-\mathrm{i}Ht}$ coming from the time evolution of operators.

Matsubara Greens function are defined as

$$G_{\alpha_1\alpha_2}(\tau_1, \tau_2) = -\left\langle T_\tau(c_{\alpha_1}(\tau_1)c^\dagger_{\alpha_2}(\tau_2))\right\rangle \tag{2.61}$$

with:

- $c_\alpha, c^\dagger_\alpha$ fermionic creation/annihilation operators of quantum states α in the Heisenberg time-evolution picture $\hat{A}(\tau) = e^{\tau H}\hat{A}e^{-\tau H}$
- $\langle\cdot\rangle = \mathrm{Tr}(r\hat{h}o\cdot)$ the thermal expectation value with statistical operator $\hat{\rho} = {}^{e^{-\beta H}}/_{Z}$ with partition function Z and Hamiltonian H

- Time-ordering operator

$$T_\tau(A(\tau)B(\tau')) = \Theta(\tau-\tau')A(\tau)B(\tau') \pm \Theta(\tau'-\tau)B(\tau')A(\tau) \quad (2.62)$$

$$= \begin{cases} A(\tau)B(\tau') & \text{if } \tau < \tau' \\ B(\tau')A(\tau) & \text{if } \tau' < \tau \end{cases} \quad (2.63)$$

Thermal equilibrium: Green's function only depends on time differences $\tau_1 - \tau_2$, so can work with a single time $\tau = \tau_1 - \tau_2$, shifting $\tau_2 = 0$. Fermionic Matsubara Green's functions are antiperiodic in time with periodicity β. For $-\beta < 0 < 0$, cyclic properties of trace tells:

$$G(\tau) = -G(\tau+\beta) \quad (2.64)$$

Restrict to interval $0 < \tau < \beta$. This means that there is a Fourier expansion with discrete frequencies $\omega_n = {}^{(2n+1)\pi}/_{\beta}$:

$$G(\mathrm{i}\omega_n) = \int_0^\beta \mathrm{d}\tau G(\tau) e^{\mathrm{i}\omega_n \tau} \quad (2.65)$$

and

$$G(\tau) = \frac{1}{\beta}\sum_n G(\mathrm{i}\omega_n) e^{-\mathrm{i}\omega_n \tau} \quad (2.66)$$

Spatial dependence $\alpha = \mathbf{R}$. In lattice context (translationally invariant, G only depends on $\mathbf{R}_1 - \mathbf{R}_2$), can transform between real-space and crystal momentum representation as

$$G(\mathbf{k}, \tau) = \sum_i G(\mathbf{R}_1) e^{\mathrm{i}\mathbf{k}\mathbf{R}_j} \quad (2.67)$$

and

$$G(\mathbf{r}) = \frac{1}{N_\mathbf{k}}\sum_\mathbf{k} G(\mathbf{k}) e^{-\mathrm{i}\mathbf{k}\mathbf{r}} \quad (2.68)$$

Can get the retarded GF $G^R_{AB}(\omega)$ by analytic continuation:

$$G^R_{AB}(\omega) = G_{AB}(\mathrm{i}\omega_n \to \omega + \mathrm{i}\eta) \quad (2.69)$$

Connection to experimental observables

What is the eta there?

Spectral representation of Matsubara and retarded GF

How to get real frequency information from Matsubara GF?

Dyson Equation

Dyson equation:

$$\mathcal{G}_\sigma(\mathbf{k}, i\omega_n) = \frac{\mathcal{G}^0_\sigma(\mathbf{k}, i\omega_n)}{1 - \mathcal{G}^0_\sigma(\mathbf{k}, i\omega_n)\Sigma_\sigma(\mathbf{k}, i\omega_n)} = \frac{1}{i\omega_n - \xi_{\mathbf{k}-\Sigma_\sigma(\mathbf{k}, i\omega_n)}} \tag{2.70}$$

Anderson Impurity Model

DMFT

Nambu-Gorkov Green's Functions

To describe superconductivity,

Order parameter can be chosen as the anomalous GF:

$$\Psi = F^{\text{loc}}(\tau = 0^-) \tag{2.71}$$

More general introduction into NG GFs, how they look like, what they describe etc.

DMFT with NG GFs as tool of approximations

2.5 Quantum Metric

Topic in quantum materials: quantum geometry and its influence on a many (quantum) material properties [22]. First (?) example: the Integer quantum Hall effect [48] that was explained by Thouless et al. to be a consequence of the unique topology of the ground state of the electron [49].

Concept of quantum geometry first formulated in 1980 by Provost and Vallee [50].

Parameter dependent Hamiltonian $\{H(\lambda)\}$, smooth dependence on parameter $\lambda = (\lambda_1, \lambda_2, ...) \in \mathcal{M}$ (base manifold)

Hamiltonian acts on parametrized Hilbert space $\mathcal{H}(\lambda)$

Eigenenergies $E_n(\lambda)$, eigenstates $|\phi_n(\lambda)\rangle$

System state $|\psi(\lambda)\rangle$ is linear combination of $|\psi_n(\lambda)\rangle$ at every point in $\mathcal{M}$

Infinitesimal variation of the parameter $d\lambda$:

Dont get it here

$$ds^2 = ||\psi(\lambda+d\lambda) - (\lambda)||^2 = \langle \delta\psi | \, \delta\psi \rangle = \langle \partial_\mu \psi | \, \partial_\nu \psi \rangle \, d\lambda^\mu \, d\lambda^\nu = (\gamma_{\mu\nu} + i\sigma_{\mu\nu}) \, d\lambda^\mu \, d\lambda^\nu \tag{2.72}$$

Last part is splitting up into real and imaginary part

Recently, the Quantum Geometric Tensor (and in turn the quantum metric) was measured [51].

Quantum Metric and Superfluid Weight

In the context of superconductivity:
[21, 31, 52]

Write up notes about quantum metric and superfluid weight

Dressed Graphene Model 3

This thesis concerned with a specific model. Idea: Graphene with an added orbital on one of the lattice site with a low hopping, as to provide a flat band. I will call this model dressed Graphene from here on. This chapter reviews the lattice structure in section 3.1.

Write introduction to the model and what is done in this chapter

Connection with Niklas/Siheeon paper on dressed Graphene

3.1 Lattice Structure

Monolayer graphene forms a honeycomb lattice [53], which is a hexagonal Bravais lattice with a two atom basis, as can be seen in fig. 3.1a. The primitive lattice vectors of the hexagonal lattice are:

$$\mathbf{a}_1 = \frac{a}{2}\begin{pmatrix} 1 \\ \sqrt{3} \end{pmatrix}, \ \mathbf{a}_2 = \frac{a}{2}\begin{pmatrix} 1 \\ -\sqrt{3} \end{pmatrix} \tag{3.1}$$

with lattice constant $a = \sqrt{3}a_0 \approx 2.46\,\text{Å}$, using the nearest-neighbour distance a_0. The vectors to the nearest-neighbor atoms B_i $(i = 1, 2, 3,)$ from atom A are

clear up NN vectors

$$\delta_{AB,1} = \begin{pmatrix} 0 \\ \frac{a}{\sqrt{3}} \end{pmatrix}, \ \delta_{AB,2} = \begin{pmatrix} \frac{a}{2} \\ -\frac{a}{2\sqrt{3}} \end{pmatrix}, \ \delta_{AB,3} = \begin{pmatrix} -\frac{a}{2} \\ -\frac{a}{2\sqrt{3}} \end{pmatrix} \tag{3.2}$$

and the vectors to the nearest-neighbor atoms A_i $(i = 1, 2, 3,)$ from atom B are

$$\delta_{BA,1} = \begin{pmatrix} 0 \\ -\frac{a}{\sqrt{3}} \end{pmatrix}, \ \delta_{BA,2} = \begin{pmatrix} -\frac{a}{2} \\ \frac{a}{2\sqrt{3}} \end{pmatrix}, \ \delta_{BA,3} = \begin{pmatrix} \frac{a}{2} \\ \frac{a}{2\sqrt{3}} \end{pmatrix}. \tag{3.3}$$

The vectors between the Graphene A atom and the six neighbours on the same sub lattice are: The primitive reciprocal lattice vectors $\mathbf{b}_1$, $\mathbf{b}_2$ fulfill

$$\mathbf{a}_1 \cdot \mathbf{b}_1 = \mathbf{a}_2 \cdot \mathbf{b}_2 = 2\pi \tag{3.4}$$

$$\mathbf{a}_1 \cdot \mathbf{b}_2 = \mathbf{a}_2 \cdot \mathbf{b}_1 = 0\,, \tag{3.5}$$

(a) (b)

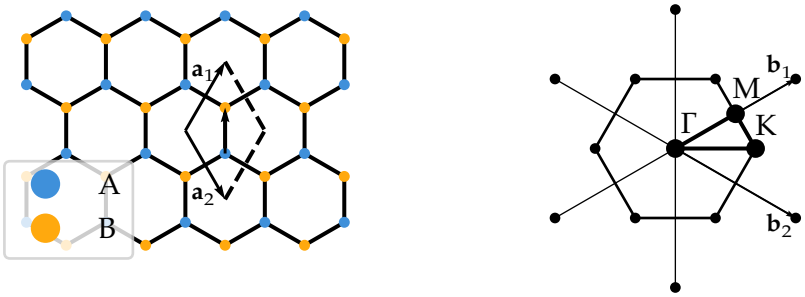

Figure 3.1 – (a) Graphene lattice structure and (b) Brilluoin zone created using lattpy [**Jones_lattpy_2022**]

so we have:

$$\mathbf{b}_1 = \frac{2\pi}{a}\begin{pmatrix} 1 \\ \frac{1}{\sqrt{3}} \end{pmatrix}, \ \mathbf{b}_2 = \frac{2\pi}{a}\begin{pmatrix} 1 \\ -\frac{1}{\sqrt{3}} \end{pmatrix} \tag{3.6}$$

The first Brilluoin zone of the hexagonal lattice is shown in fig. 3.1b, with the points of high symmetry

$$\Gamma = \begin{pmatrix} 0 \\ 0 \end{pmatrix}, \ \mathrm{M} = \frac{\pi}{a}\begin{pmatrix} 1 \\ \frac{1}{\sqrt{3}} \end{pmatrix}, \ \mathrm{K} = \frac{4\pi}{3a}\begin{pmatrix} 1 \\ 0 \end{pmatrix} . \tag{3.7}$$

3.2 Dressed Graphene Model

The model I am concerned with in this thesis consists of a Hubbard Hamiltonian (as introduced in section 2.2) on a Graphene lattice, with one additional atom at one of the two sites in a unit cell, which I will call X. This is shown in fig. 3.2. The kinetic term is

$$H_0 = -t \sum_{\langle ij \rangle, \sigma} c^{(\mathrm{A}),\dagger}_{i,\sigma} c^{(\mathrm{B})}_{j,\sigma} + V \sum_{i,\sigma\sigma'} d^{\dagger}_{i,\sigma} c^{(\mathrm{A})}_{i,\sigma'} + \mathrm{h.c.} \tag{3.8}$$

with

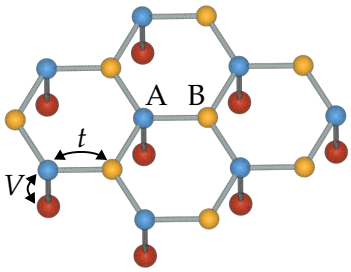

Figure 3.2 – Lattice structure of decorated graphene honeycomb lattice. with impurity X hybridized to sublattice site A. Only hopping t between sublattices A and B as well as V between X and A exist. Created using VESTA [54].

- d - operators on the X atom
- $c^{(\epsilon)}$ - operators on the graphene sites ($\epsilon = \mathrm{A}, \mathrm{B}$)
- t - nearest neighbour hopping between Graphene sites
- V - hopping between X and Graphene A sites.

The notation using different letters for the sites connects intuitively to the physical picture, but it is more economical and in line with the notation for mean field-theory established in section 2.2 to write the Hamiltonian using a sublattice index

$$\alpha = 1, 2, 3 \tag{3.9}$$

with $1 \mathrel{\widehat{=}} \mathrm{Gr_A}$, $2 \mathrel{\widehat{=}} \mathrm{Gr_B}$, $3 \mathrel{\widehat{=}} \mathrm{X}$. Then we can write the non-interacting term as

$$H_0 = -t \sum_{\langle ij \rangle, \sigma} c^\dagger_{\alpha=1,i,\sigma} c_{\alpha=2,j,\sigma} + V \sum_{i,\sigma} c^\dagger_{\alpha=1,i,\sigma} c_{\alpha=3,i,\sigma} + \mathrm{h.c.} \tag{3.10}$$

The (attractive) Hubbard interaction has the following form:

$$H_{\mathrm{int}} = -\sum_{i\alpha} U_\alpha c^\dagger_{i\alpha\uparrow} c^\dagger_{i\alpha\downarrow} c_{i\alpha\downarrow} c_{i\alpha\uparrow} \, . \tag{3.11}$$

Fourier trafo :

Clean up the section from here

Fourier trafo with orbital positions

$$-t\sum_{\langle ij\rangle,\sigma} c_{i,\sigma}^{(\mathrm{A}),\dagger} c_{j,\sigma}^{(\mathrm{B})} = -t\sum_{i,\delta_{\mathrm{AB}},\sigma} c_{i,\sigma}^{(\mathrm{A})\dagger} c_{i+\delta_{\mathrm{AB}},\sigma}^{(\mathrm{B})} \tag{3.12}$$

$$= -\frac{t}{N^2}\sum_{i,\sigma}\sum_{\mathbf{k},\mathbf{k}',\delta_{\mathrm{AB}}} \left(e^{-\mathrm{i}\mathbf{k}\mathbf{r}_i} c_{\mathbf{k},\sigma}^{(\mathrm{A})\dagger}\right)\left(e^{\mathrm{i}\mathbf{k}'\mathbf{r}_i+\delta_{AB}} c_{\mathbf{k}',\sigma}^{(B)}\right) \tag{3.13}$$

$$= -\frac{t}{N^2}\sum_{\mathbf{k},\mathbf{k}',\delta_{\mathrm{AB}},\sigma} c_{\mathbf{k},\sigma}^{(\mathrm{A})\dagger} c_{\mathbf{k}',\sigma}^{(\mathrm{B})} e^{\mathrm{i}\mathbf{k}'\delta_{\mathrm{AB}}} \sum_i e^{-\mathrm{i}\mathbf{k}\mathbf{r}_i} e^{\mathrm{i}\mathbf{k}'\mathbf{r}_i} \tag{3.14}$$

$$= -\frac{t}{N^2}\sum_{\mathbf{k},\mathbf{k}',\sigma} c_{\mathbf{k},\sigma}^{(\mathrm{A})\dagger} c_{\mathbf{k}',\sigma}^{(\mathrm{B})} \sum_{\delta_{\mathrm{AB}}} e^{\mathrm{i}\mathbf{k}'\delta_{\mathrm{AB}}} \left(N^2\delta_{\mathbf{k},\mathbf{k}'}\right) \tag{3.15}$$

$$= -t\sum_{\mathbf{k},\sigma} c_{\mathbf{k},\sigma}^{(\mathrm{A})\dagger} c_{\mathbf{k},\sigma}^{(\mathrm{B})} \sum_{\delta_{\mathrm{AB}}} e^{\mathrm{i}\mathbf{k}\delta_{AB}} = \sum_{\mathbf{k},\sigma} f_{\mathbf{k}} c_{\mathbf{k},\sigma}^{(\mathrm{A})\dagger} c_{\mathbf{k},\sigma}^{(\mathrm{B})} \tag{3.16}$$

Clear up definition NN vectors and results

$$\mathbf{k}\cdot\delta_{\mathbf{AA},\mathbf{1}} = \begin{pmatrix} k_x \\ k_y \end{pmatrix}\cdot\begin{pmatrix} 1 \\ \sqrt{3} \end{pmatrix} = k_x + \sqrt{3}k_y \tag{3.17}$$

$$f_{\mathbf{k}} = -t\sum_{\delta_{AB}} e^{\mathrm{i}\mathbf{k}\delta_{AB}} \tag{3.18}$$

$$= -t_{\mathrm{Gr}}\left(e^{\mathrm{i}\frac{a}{\sqrt{3}}k_y} + e^{\mathrm{i}\frac{a}{2\sqrt{3}}(\sqrt{3}k_x-k_y)} + e^{\mathrm{i}\frac{a}{2\sqrt{3}}(-\sqrt{3}k_x-k_y)}\right) \tag{3.19}$$

$$= -t_{\mathrm{Gr}}\left(e^{\mathrm{i}\frac{a}{\sqrt{3}}k_y} + e^{-\mathrm{i}\frac{a}{2\sqrt{3}}k_y}\left(e^{\mathrm{i}\frac{a}{2}k_x} + e^{-\mathrm{i}\frac{a}{2}k_x}\right)\right) \tag{3.20}$$

$$= -t_{\mathrm{Gr}}\left(e^{\mathrm{i}\frac{a}{\sqrt{3}}k_y} + 2e^{-\mathrm{i}\frac{a}{2\sqrt{3}}k_y}\cos\left(\frac{a}{2}k_x\right)\right) \tag{3.21}$$

We have $\delta_{\mathrm{BA},i} = -\delta_{\mathrm{AB},i}$, so

$$-t\sum_{\delta_{BA}} e^{\mathrm{i}\mathbf{k}\delta_{BA}} = -t\sum_{\delta_{AB}} e^{-\mathrm{i}\mathbf{k}\delta_{AB}} = \left(-t\sum_{\delta_{AB}} e^{\mathrm{i}\mathbf{k}\delta_{AB}}\right)^* = f_{\mathbf{k}}^* \tag{3.22}$$

which then gives

$$H_0 = \sum_{\mathbf{k},\sigma,\sigma'} \begin{pmatrix} c_{k,\sigma}^{A,\dagger} & c_{k,\sigma}^{B,\dagger} & d_{k,\sigma}^{\dagger} \end{pmatrix} \begin{pmatrix} 0 & f_{\mathbf{k}} & V \\ f_{\mathbf{k}}^* & 0 & 0 \\ V & 0 & 0 \end{pmatrix} \begin{pmatrix} c_{k,\sigma}^{A} \\ c_{k,\sigma}^{B} \\ d_{k,\sigma} \end{pmatrix} \tag{3.23}$$

The band structure for the non-interacting dressed graphene model is easily obtained by diagonalising the matrix in eq. (3.23). This was done in fig. 3.3.

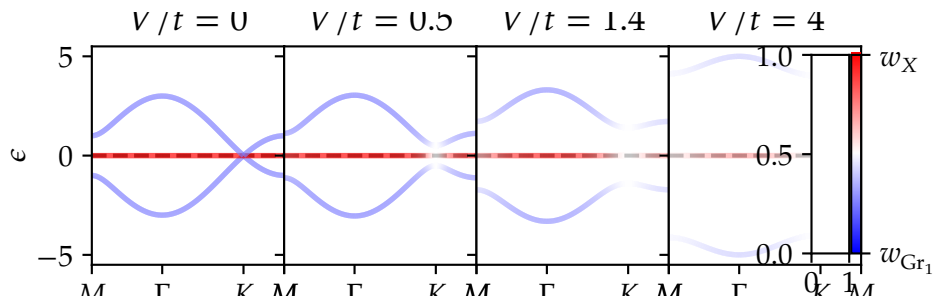

Figure 3.3 – Bands of the non-interacting dressed Graphene model

4 Superconducting Length Scales

Computational Implementation and Data Availability

A

BCS code

The implementation of BCS self-consistency with finite momentum was done by me from ground-up. The code and documentation is available at github.com/Ruberhauptmann/quant-met. The implementation relies on the work of many contributors of packages in Pythons ecosystem, most important among them NumPy [55], SciPy [56], Matplotlib [57], Pandas [58, 59] and Parasweep [60].

All the data and instructions on how to reproduce the calculations and analysis is available at osf.io/sajeh/. For reproducibility, Datalad [61] is used.

DMFT

DMFT loop using TRIQS [62], it can also be found under osf.io/sajeh/.

Bibliography

[1] United Nations. *International Year of Quantum Science and Technology, 2025*. May 10, 2024. URL: https://docs.un.org/A/78/L.70 (visited on 02/18/2025) (cit. on p. 1).

[2] H. K. Onnes. "Further Experiments with Liquid Helium. G. On the Electrical Resistance of Pure Metals, Etc. VI. On the Sudden Change in the Rate at Which the Resistance of Mercury Disappears." In: *Through Measurement to Knowledge: The Selected Papers of Heike Kamerlingh Onnes 1853–1926*. Ed. by K. Gavroglu and Y. Goudaroulis. Dordrecht: Springer Netherlands, 1991, pp. 267–272. ISBN: 978-94-009-2079-8. DOI: 10.1007/978-94-009-2079-8_17 (cit. on p. 1).

[3] J. G. Bednorz and K. A. Müller. "Possible High Tc Superconductivity in the Ba—La—Cu—O System". In: *Zeitschrift für Physik B Condensed Matter* 64.2 (June 1, 1986), pp. 189–193. ISSN: 1431-584X. DOI: 10.1007/BF01303701 (cit. on p. 1).

[4] S.-i. Uchida et al. "High Tc Superconductivity of La-Ba-Cu Oxides". In: *Japanese Journal of Applied Physics* 26 (1A Jan. 1, 1987), p. L1. ISSN: 1347-4065. DOI: 10.1143/JJAP.26.L1 (cit. on p. 1).

[5] D. Rybicki et al. "Perspective on the Phase Diagram of Cuprate High-Temperature Superconductors". In: *Nature Communications* 7.1 (May 6, 2016), p. 11413. ISSN: 2041-1723. DOI: 10.1038/ncomms11413 (cit. on p. 1).

[6] P. A. Rinck. *Magnetic Resonance in Medicine - A Critical Introduction*. ISBN: 978-628-01-2260-1. URL: http://www.magnetic-resonance.org/ (cit. on p. 1).

[7] A. Tollestrup and E. Todesco. "The Development of Superconducting Magnets for Use in Particle Accelerators: From the Tevatron to the LHC". In: *Reviews of Accelerator Science and Technology* 1.01 (2008), pp. 185–210 (cit. on p. 1).

[8] L. Rossi. "Particle Accelerators and Cuprate Superconductors". In: *Physica C: Superconductivity and its Applications* 614 (Nov. 15, 2023), p. 1354360. ISSN: 0921-4534. DOI: 10.1016/j.physc.2023.1354360 (cit. on p. 1).

[9] K. Irwin and G. Hilton. "Transition-Edge Sensors". In: *Cryogenic Particle Detection*. Ed. by C. Enss. Berlin, Heidelberg: Springer, 2005, pp. 63–150. ISBN: 978-3-540-31478-3. DOI: 10.1007/10933596_3 (cit. on p. 1).

[10] M. I. Faley et al. "High-Tc SQUID Biomagnetometers". In: *Superconductor Science and Technology* 30.8 (July 2017), p. 083001. ISSN: 0953-2048. DOI: 10.1088/1361-6668/aa73ad (cit. on p. 1).

[11] A. M. Klushin et al. "Present and Future of High-Temperature Superconductor Quantum-Based Voltage Standards". In: *IEEE Instrumentation & Measurement Magazine* 23.2 (Apr. 2020), pp. 4–12. ISSN: 1941-0123. DOI: 10.1109/MIM.2020.9062678 (cit. on p. 1).

[12] B. D. Josephson. "Possible New Effects in Superconductive Tunnelling". In: *Physics Letters* 1.7 (July 1, 1962), pp. 251–253. ISSN: 0031-9163. DOI: 10.1016/0031-9163(62)91369-0 (cit. on p. 1).

[13] Y. Cao et al. "Unconventional Superconductivity in Magic-Angle Graphene Superlattices". In: *Nature* 556.7699 (Apr. 2018), pp. 43–50. ISSN: 1476-4687. DOI: 10.1038/nature26160 (cit. on p. 2).

[14] P. Coleman. *Introduction to Many-Body Physics*. Cambridge University Press, Nov. 2015. ISBN: 978-0-521-86488-6. DOI: 10.1017/CBO9781139020916 (cit. on pp. 3, 12–14, 17).

[15] M. Tinkham. *Introduction to Superconductivity*. 2. ed. International Series in Pure and Applied Physics. New York: McGraw-Hill, 1996. 454 pp. ISBN: 978-0-07-064878-4 (cit. on pp. 3, 11, 12).

[16] H. Bruus and K. Flensberg. *Many-Body Quantum Theory in Condensed Matter Physics: An Introduction*. Oxford Graduate Texts. Oxford, New York: Oxford University Press, Nov. 11, 2004. 466 pp. ISBN: 978-0-19-856633-5 (cit. on pp. 3, 14, 17).

[17] A. I. Larkin and A. A. Varlamov. *Theory of Fluctuations in Superconductors*. Oxford Science Publications 127. Oxford Oxford: Clarendon Press Oxford University Press, 2005. ISBN: 978-0-19-852815-9 (cit. on p. 3).

[18] K. H. Bennemann and J. B. Ketterson, eds. *Superconductivity*. Berlin, Heidelberg: Springer Berlin Heidelberg, 2008. ISBN: 978-3-540-73252-5. DOI: 10.1007/978-3-540-73253-2 (cit. on p. 3).

[19] A. Beekman, L. Rademaker, and J. van Wezel. "An Introduction to Spontaneous Symmetry Breaking". In: *SciPost Physics Lecture Notes* (Dec. 4, 2019), p. 011. ISSN: 2590-1990. DOI: 10.21468/SciPostPhysLectNotes.11 (cit. on p. 3).

[20] N. Witt et al. "Bypassing the Lattice BCS–BEC Crossover in Strongly Correlated Superconductors through Multiorbital Physics". In: *npj Quantum Materials* 9.1 (Dec. 10, 2024), pp. 1–10. ISSN: 2397-4648. DOI: 10.1038/s41535-024-00706-7 (cit. on pp. 3, 10).

[21] S. Peotta and P. Törmä. "Superfluidity in Topologically Nontrivial Flat Bands". In: *Nature Communications* 6.1 (Nov. 20, 2015), p. 8944. ISSN: 2041-1723. DOI: 10.1038/ncomms9944 (cit. on pp. 4, 12, 16, 21).

[22] J. Yu et al. *Quantum Geometry in Quantum Materials*. Dec. 30, 2024. DOI: 10.48550/arXiv.2501.00098. Pre-published (cit. on pp. 4, 20).

[23] E. Noether. "Invariante Variationsprobleme". In: *Nachrichten von der Gesellschaft der Wissenschaften zu Göttingen, Mathematisch-Physikalische Klasse* 1918 (1918), pp. 235–257. URL: https://eudml.org/doc/59024 (visited on 12/10/2024) (cit. on p. 4).

[24] L. D. Landau. "On the Theory of Phase Transitions". In: *Zhurnal Eksperimental'noi i Teoreticheskoi Fiziki* 7 (1937). Ed. by D. ter Haar, pp. 19–32. DOI: 10.1016/B978-0-08-010586-4.50034-1 (cit. on p. 4).

[25] V. L. Ginzburg and L. D. Landau. "On the Theory of Superconductivity". In: *Zhurnal Eksperimental'noi i Teoreticheskoi Fiziki* 20 (1950). Ed. by D. ter Haar, pp. 1064–1082. DOI: 10.1016/b978-0-08-010586-4.50078-x (cit. on pp. 5, 7).

[26] A. Q. Chen et al. "Finite Momentum Cooper Pairing in Three-Dimensional Topological Insulator Josephson Junctions". In: *Nature Communications* 9.1 (Aug. 28, 2018), p. 3478. ISSN: 2041-1723. DOI: 10.1038/s41467-018-05993-w (cit. on p. 10).

[27] P. Wan et al. "Orbital Fulde–Ferrell–Larkin–Ovchinnikov State in an Ising Superconductor". In: *Nature* 619.7968 (July 2023), pp. 46–51. ISSN: 1476-4687. DOI: 10.1038/s41586-023-05967-z (cit. on p. 10).

[28] N. F. Q. Yuan and L. Fu. "Supercurrent Diode Effect and Finite-Momentum Superconductors". In: *Proceedings of the National Academy of Sciences* 119.15 (Apr. 12, 2022), e2119548119. DOI: 10.1073/pnas.2119548119 (cit. on p. 10).

[29] J. Bardeen. "Critical Fields and Currents in Superconductors". In: *Reviews of Modern Physics* 34.4 (Oct. 1, 1962), pp. 667–681. DOI: 10.1103/RevModPhys.34.667 (cit. on p. 11).

[30] K. Xu, P. Cao, and J. R. Heath. "Achieving the Theoretical Depairing Current Limit in Superconducting Nanomesh Films". In: *Nano Letters* 10.10 (Oct. 13, 2010), pp. 4206–4210. ISSN: 1530-6984. DOI: 10.1021/nl102584j (cit. on p. 11).

[31] L. Liang et al. "Band Geometry, Berry Curvature, and Superfluid Weight". In: *Physical Review B* 95.2 (Jan. 27, 2017), p. 024515. DOI: 10.1103/PhysRevB.95.024515 (cit. on pp. 12, 21).

[32] L. C. Hebel and C. P. Slichter. "Nuclear Relaxation in Superconducting Aluminum". In: *Physical Review* 107.3 (Aug. 1, 1957), pp. 901–902. DOI: 10.1103/PhysRev.107.901 (cit. on p. 13).

[33] L. C. Hebel and C. P. Slichter. "Nuclear Spin Relaxation in Normal and Superconducting Aluminum". In: *Physical Review* 113.6 (Mar. 15, 1959), pp. 1504–1519. DOI: 10.1103/PhysRev.113.1504 (cit. on p. 13).

[34] I. Giaever and K. Megerle. "Study of Superconductors by Electron Tunneling". In: *Physical Review* 122.4 (May 15, 1961), pp. 1101–1111. DOI: 10.1103/PhysRev.122.1101 (cit. on p. 13).

[35] F. London. "A New Conception of Supraconductivity". In: *Nature* 140.3549 (Nov. 1, 1937), pp. 793–796. ISSN: 1476-4687. DOI: 10.1038/140793a0 (cit. on p. 13).

[36] X. Zhou et al. "High-Temperature Superconductivity". In: *Nature Reviews Physics* 3.7 (July 2021), pp. 462–465. ISSN: 2522-5820. DOI: 10.1038/s42254-021-00324-3 (cit. on p. 13).

[37] J. Hubbard and B. H. Flowers. "Electron Correlations in Narrow Energy Bands". In: *Proceedings of the Royal Society of London. Series A. Mathematical and Physical Sciences* 276.1365 (Nov. 26, 1963), pp. 238–257. DOI: 10.1098/rspa.1963.0204 (cit. on p. 13).

[38] J. Kanamori. "Electron Correlation and Ferromagnetism of Transition Metals". In: *Progress of Theoretical Physics* 30.3 (Sept. 1, 1963), pp. 275–289. ISSN: 0033-068X. DOI: 10.1143/PTP.30.275 (cit. on p. 13).

[39] M. C. Gutzwiller. "Effect of Correlation on the Ferromagnetism of Transition Metals". In: *Physical Review Letters* 10.5 (Mar. 1, 1963), pp. 159–162. DOI: 10.1103/PhysRevLett.10.159 (cit. on p. 13).

[40] F. C. Zhang and T. M. Rice. "Effective Hamiltonian for the Superconducting Cu Oxides". In: *Physical Review B* 37.7 (Mar. 1, 1988), pp. 3759–3761. DOI: 10.1103/PhysRevB.37.3759 (cit. on p. 13).

[41] M. Qin et al. "The Hubbard Model: A Computational Perspective". In: *Annual Review of Condensed Matter Physics* 13 (Volume 13, 2022 Mar. 10, 2022), pp. 275–302. ISSN: 1947-5454, 1947-5462. DOI: 10.1146/annurev-conmatphys-090921-033948 (cit. on p. 13).

[42] R. Micnas, J. Ranninger, and S. Robaszkiewicz. "Superconductivity in Narrow-Band Systems with Local Nonretarded Attractive Interactions". In: *Reviews of Modern Physics* 62.1 (Jan. 1, 1990), pp. 113–171. DOI: 10.1103/RevModPhys.62.113 (cit. on p. 14).

[43] K.-E. Huhtinen. "Superconductivity and Normal State Properties in Flat Bands". Aalto University, 2023. URL: https://aaltodoc.aalto.fi/handle/123456789/119970 (visited on 11/27/2024) (cit. on p. 14).

[44] J. J. Kinnunen et al. "The Fulde–Ferrell–Larkin–Ovchinnikov State for Ultracold Fermions in Lattice and Harmonic Potentials: A Review". In: *Reports on Progress in Physics* 81.4 (Feb. 2018), p. 046401. ISSN: 0034-4885. DOI: 10.1088/1361-6633/aaa4ad (cit. on p. 15).

[45] Q. Chen et al. "When Superconductivity Crosses over: From BCS to BEC". In: *Reviews of Modern Physics* 96.2 (May 23, 2024), p. 025002. DOI: 10.1103/RevModPhys.96.025002 (cit. on p. 17).

[46] E. Pavarini et al., eds. *Dynamical Mean-Field Theory of Correlated Electrons*. Schriften Des Forschungszentrums Jülich Reihe Modeling and Simulation Band/volume 12. Jülich: Forschungszentrum Jülich, Zentralbibliothek, Verlag, 2022. 1 p. ISBN: 978-3-95806-619-9 (cit. on p. 17).

[47] A. Georges et al. "Dynamical Mean-Field Theory of Strongly Correlated Fermion Systems and the Limit of Infinite Dimensions". In: *Reviews of Modern Physics* 68.1 (Jan. 1, 1996), pp. 13–125. DOI: 10.1103/RevModPhys.68.13 (cit. on p. 17).

[48] K. v. Klitzing, G. Dorda, and M. Pepper. "New Method for High-Accuracy Determination of the Fine-Structure Constant Based on Quantized Hall Resistance". In: *Physical Review Letters* 45.6 (Aug. 11, 1980), pp. 494–497. DOI: 10.1103/PhysRevLett.45.494 (cit. on p. 20).

[49] D. J. Thouless et al. "Quantized Hall Conductance in a Two-Dimensional Periodic Potential". In: *Physical Review Letters* 49.6 (Aug. 9, 1982), pp. 405–408. DOI: 10.1103/PhysRevLett.49.405 (cit. on p. 20).

[50] J. P. Provost and G. Vallee. "Riemannian Structure on Manifolds of Quantum States". In: *Communications in Mathematical Physics* 76.3 (Sept. 1, 1980), pp. 289–301. ISSN: 1432-0916. DOI: 10.1007/BF02193559 (cit. on p. 20).

[51] M. Kang et al. "Measurements of the Quantum Geometric Tensor in Solids". In: *Nature Physics* 21.1 (Jan. 2025), pp. 110–117. ISSN: 1745-2481. DOI: 10.1038/s41567-024-02678-8 (cit. on p. 20).

[52] P. Törmä, S. Peotta, and B. A. Bernevig. "Superconductivity, Superfluidity and Quantum Geometry in Twisted Multilayer Systems". In: *Nature Reviews Physics* 4.8 (Aug. 2022), pp. 528–542. ISSN: 2522-5820. DOI: 10.1038/s42254-022-00466-y (cit. on p. 21).

[53] G. Yang et al. "Structure of Graphene and Its Disorders: A Review". In: *Science and Technology of Advanced Materials* 19.1 (Aug. 29, 2018), pp. 613–648. ISSN: 1468-6996. DOI: 10.1080/14686996.2018.1494493 (cit. on p. 22).

[54] K. Momma and F. Izumi. "*VESTA 3* for Three-Dimensional Visualization of Crystal, Volumetric and Morphology Data". In: *Journal of Applied Crystallography* 44.6 (Dec. 1, 2011), pp. 1272–1276. ISSN: 0021-8898. DOI: 10.1107/S0021889811038970 (cit. on p. 24).

[55] C. R. Harris et al. "Array Programming with NumPy". In: *Nature* 585.7825 (Sept. 2020), pp. 357–362. ISSN: 1476-4687. DOI: 10.1038/s41586-020-2649-2 (cit. on p. 28).

[56] P. Virtanen et al. "SciPy 1.0: Fundamental Algorithms for Scientific Computing in Python". In: *Nature Methods* 17.3 (Mar. 2020), pp. 261–272. ISSN: 1548-7105. DOI: 10.1038/s41592-019-0686-2 (cit. on p. 28).

[57] J. D. Hunter. "Matplotlib: A 2D Graphics Environment". In: *Computing in Science & Engineering* 9.3 (May 2007), pp. 90–95. ISSN: 1558-366X. DOI: 10.1109/MCSE.2007.55 (cit. on p. 28).

[58] W. McKinney. "Data Structures for Statistical Computing in Python". In: Python in Science Conference. Austin, Texas, 2010, pp. 56–61. DOI: 10.25080/Majora-92bf1922-00a (cit. on p. 28).

[59] T. pandas development team. *Pandas-Dev/Pandas: Pandas*. Version v2.2.3. Zenodo, Sept. 20, 2024. DOI: 10.5281/ZENODO.3509134 (cit. on p. 28).

[60] E. Bach. "Parasweep: A Template-Based Utility for Generating, Dispatching, and Post-Processing of Parameter Sweeps". In: *SoftwareX* 13 (Jan. 1, 2021), p. 100631. ISSN: 2352-7110. DOI: 10.1016/j.softx.2020.100631 (cit. on p. 28).

[61] Y. O. Halchenko et al. "DataLad: Distributed System for Joint Management of Code, Data, and Their Relationship". In: *Journal of Open Source Software* 6.63 (July 1, 2021), p. 3262. ISSN: 2475-9066. DOI: 10.21105/joss.03262 (cit. on p. 28).

[62] O. Parcollet et al. "TRIQS: A Toolbox for Research on Interacting Quantum Systems". In: *Computer Physics Communications* 196 (Nov. 1, 2015), pp. 398–415. ISSN: 0010-4655. DOI: 10.1016/j.cpc.2015.04.023 (cit. on p. 28).

Not cited

[63] J. Bardeen, L. N. Cooper, and J. R. Schrieffer. "Theory of Superconductivity". In: *Physical Review* 108.5 (Dec. 1, 1957), pp. 1175–1204. DOI: 10.1103/PhysRev.108.1175.

[64] U. of Chicago. *Annual Register*. 1893-1930., 1896. 462 pp.

[65] L. N. Cooper. "Bound Electron Pairs in a Degenerate Fermi Gas". In: *Physical Review* 104.4 (Nov. 15, 1956), pp. 1189–1190. DOI: 10.1103/PhysRev.104.1189.

[66] T. Hazra, N. Verma, and M. Randeria. "Bounds on the Superconducting Transition Temperature: Applications to Twisted Bilayer Graphene and Cold Atoms". In: *Physical Review X* 9.3 (Sept. 17, 2019), p. 031049. DOI: 10.1103/PhysRevX.9.031049.

[67] W. Meissner and R. Ochsenfeld. "Ein neuer Effekt bei Eintritt der Supraleitfähigkeit". In: *Naturwissenschaften* 21.44 (Nov. 1, 1933), pp. 787–788. ISSN: 1432-1904. DOI: 10.1007/BF01504252.

Listings

List of Figures

List of Abbreviations

BCS Bardeen-Cooper-Schrieffer 3, 12

DMFT Dynamical Mean Field Theory 3, 17

BdG Bogoliubov-de Gennes 16